DEVELOPMENT AND TESTING OF A NOVEL GAMMA RAY CAMERA FOR RADIATION SURVEYING, CONTAMINATION MEASUREMENT AND RADIATION DETECTION

John A. Mason, Marc R. Looman and Adam J. Poundall
ANTECH, A. N. Technology Ltd.
Unit 6, Thames Park, Wallingford, Oxfordshire, OX10 9TA, England

Daniel Pancake and Richard Creed
Argonne National Laboratory
9700 South Cass Avenue, Lemont, IL 60439, USA

ABSTRACT

This paper records the design and operation of a novel gamma-ray camera device. The instrument combines in one detector head a sensitive and highly collimated LaBr3 scintillation detector with an optical (video) camera with controllable zoom and focus and a laser range finder. The LaBr3 detector resolution is nearly three times that of NaI. The detector is housed in an effective tungsten shield, which provides a shielding ratio of 50:1 in the forward direction and 10:1 on the sides and to the rear for incident 1,500 keV gamma-rays. The detector head is mounted on a pan/tile mechanism with a range of motion of 360 degrees (pan) and +/- 90 degrees (tilt). The detector head with pan/tilt is normally mounted on a tripod but can also be mounted on vehicles or a mobile robot for access to high dose-rate areas. A single combined power and communication cable of up to 100 metres connects the detector head to a distant operator station. This consists of a small power supply box connected to 110 or 230 VAC and a notebook computer. Operation of the detector head with all of its measuring functions is controlled from the notebook computer over Ethernet. The unit can be powered from a 24 volt battery and be controlled using wireless Ethernet for remote operation. The device is portable and can be deployed readily indoors or in the field by an operator. Software allows both automatic and manual operation and an operator can specify coordinates to search a specific position or area or a search can be conducted automatically in 4π steradians, using the full capabilities of the pan/tilt mechanism. Each gamma-ray measurement captures an entire spectrum for each incremental measurement position. From each spectrum a number of pre-set gamma-ray regions of interest corresponding to radionuclide peaks can be obtained. The unit reports the intensity (dose-rate) and activity for a variety of pre-selected radionuclides at different positions in relation to a video image. The results of Monte Carlo MCNP modelling are compared with measurements of radioactive sources.

INTRODUCTION

ANTECH RadSearch is a novel radiation detection and measurement device based on the use of a detector head, consisting of a gamma-ray detector, a video camera and a laser range finder. The detector head is mounted on a pan and tilt unit, which itself is mounted on a tripod, trolley or vehicle. The detector head and pan-tilt mechanism are connected to a remote monitoring station consisting of a small power supply unit and notebook computer. RadSearch, which is sometimes referred to as a gamma camera, is designed for radiation surveying, radioactive contamination measurement and radiation detection. RadSearch is relevant to a wide variety of applications, including radiation detection, radiation clean up, decommissioning and radioactive waste assay.

At the centre of the detector head is a one-inch lanthanum bromide (LaBr3) gamma-ray scintillation detector and photomultiplier. The LaBr3 scintillation detector has a gamma-ray energy resolution that is nearly three times that of sodium iodide (NaI) detectors. It has an energy range of between 30 keV to 2,000 keV, and an energy resolution of typically 2.5% to 3% (FWHM – full width half maximum). Gamma-ray data acquisition is achieved using an 8K channel Multi-Channel Analyser (MCA), which accumulates gamma-ray spectra for each measurement made by the detector.

Aligned with the LaBr3 detector is an optical (video) CMOS camera with controllable zoom lens, autofocus and auto-iris. The camera is employed to record video images of the areas and equipment being surveyed and measured. The zoom feature allows close-up images to be recorded of individual Scan Elements, which comprise an overall Scan Area. The distance between the detector and camera and the object being measured or scanned is determined by the use of a calibrated laser range finder (also aligned with the detector) with a range of up to 65 meters and a resolution of +/- 3mm.

The detector head is mounted on a pan and tilt mechanism with a range of motion of +/- 180 degrees pan and +/- 90 degrees tilt, giving a total solid angle of view of 4π steradians. Normally, the detector head and pan and tilt unit is mounted on a tripod, as can be seen in Figure 1. Also displayed in Figure 1 is the remote monitoring station, consisting of a rugged notebook computer and small power supply unit. Figure 2 (overleaf) is a view showing the components of the detector head.
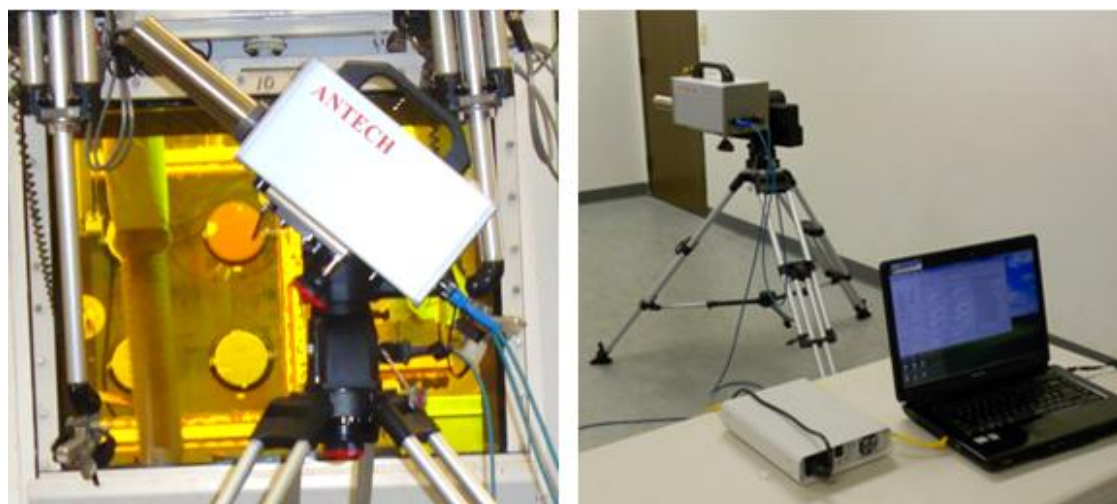

Figure 1. This figure provides two views of RadSearch, showing the detector head, pan and tilt unit and tripod. In the second view the power supply unit and notebook compute are also visible.

RadSearch is normally operated from the notebook computer, which can be located up to 100 meters from the detector head with the power supply unit. The power supply operates on either 110 or 240 VAC and provides 50 volts DC from the power supply unit to the detector head and pan tilt unit. Communication between the notebook computer and the detector head is by Ethernet. A single cable carries both 50 VDC and Ethernet. For remote operation the unit can also be powered from a 24-volt battery and can be controlled by wireless Ethernet. The RadSearch instrument is portable and the combined weight of all of the components is less than 54 kg (not including the three rugged transport cases). It can be assembled and deployed by a single person in less than 10 minutes.

In normal operation, RadSearch provides a video image of the object or surface being measured with a coloured overlay showing the distribution of radioactivity. RadSearch divides the video image into a rectangular grid consisting of a number of Scan Elements.

A gamma-ray spectrum is obtained for each Scan Element. From each measured spectrum a number of different radionuclides can be identified. The overall image consisting of all Scan Elements is called the Scan Area.

Pre-set libraries of common radionuclides are provided and the operator is able to establish other libraries with additional radionuclides, if required. A separate scan overlay (Scan Area) is generated for each radionuclide in the selected library. Each scan overlay (which is specific to a particular radionuclide) shows the relative intensity of the gamma-ray count rate for that radionuclide, distributed over all the Scan Elements of the Scan Area.

RadSearch calculates the total activity for each selected radionuclide over the Scan Area. It also determines the dose rate at the detector arising from sources distributed over the Scan Area. This data is available in a table on the notebook computer screen and is also available as a comma separated file that can be loaded into a spread-sheet for further analysis and manipulation.

RadSearch has a wide dose rate operating range from 0.003 μGy/h (μSv/h) up to 500 mGy/h (mSv/h). For Cs-137 the minimum detectible activity (MDA) is less than 1 μCi at a distance of 1 meter from the detector.
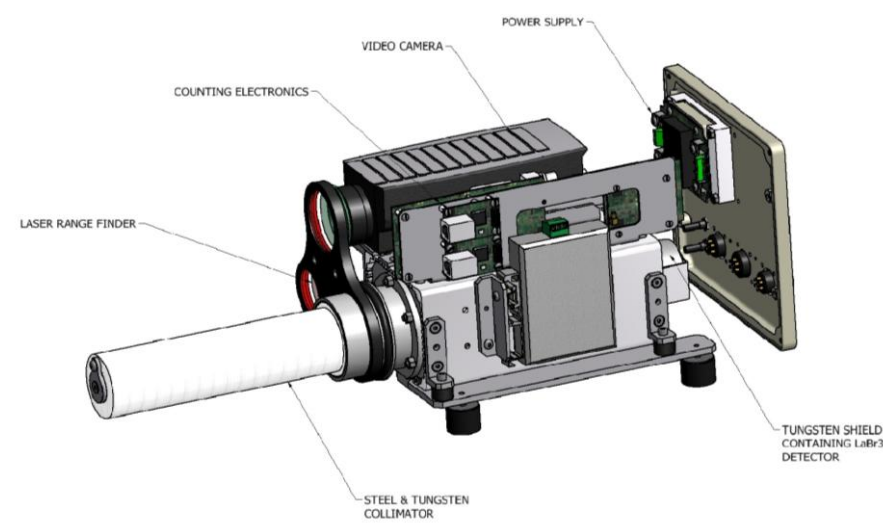

Figure 2. View of the components of the detector head.

MODELLING OF DETECTOR CHARACTERISTICS

The MCNP Monte Carlo modelling code [1] was used to model a variety of characteristics of the detector and shielding as part of the design of the instrument. The detector field of view (FOV) for different collimator options was modelled, as was the effective shielding of the tungsten shied in which the LaBr3 detector and photomultiplier are housed. The shielding was initially designed assuming incident gamma-ray energy of 1,500 keV, such that in the forward direction the shielding effectiveness was greater than a factor of 50 and at angles greater than 45 degrees a factor of 10 was achieved. While ensuring adequate detector shielding, the weight of the detector head was kept below 20 kg, with the collimating barrel detached. Two collimator options have been included in the design. The first, excluding the barrel, provides a detector field of view (detector FOV) of 18 degrees at FWHM. The second, designed for use with smaller Scan Elements, incorporates a steel and tungsten barrel with a detector FOV of 4 degrees. The results of the Monte Carlo calculation are displayed in Figure 3 for 1,500 keV gamma-ray photons.

The values for the 661.7 keV case are derived from the 1,500 keV values by using mass attenuation coefficients from Hubbell and Seltzer [2] (The tungsten alloy density is 18.7 g.cm^{-3} and the mass attenuation for 661.7 and 1,500 keV are respectively 0.0933 and 0.05 cm^2.g^{-1}). The minimum shielding factor for 661.7 keV photons from Cs-137 is a factor of 100.
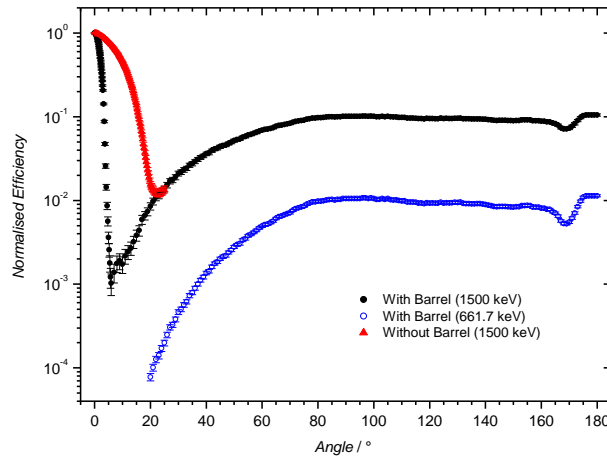

Figure 3. Normalised efficiency as a function of the angle in °. The values for the 1,500 keV cases (with and without barrel collimator) are based on Monte Carlo simulations. The shielding effectiveness for 661.7 keV photons is at least 9.24 times better than that for 1,500 keV photons.

Detector efficiency has been modelled based on the assumption of an isotropic point source placed at a distance of 25 cm from the front face of the detector and photomultiplier assembly. The result of the MCNP simulations is displayed in Figure 4. Superimposed on the curve of simulated data are experimental measurements of low activity point sources, including Ba-133, Cs-137 and Co-60. In order to further characterize the detector, the full width half maxima (FWHM) of the gamma-ray peaks determined by a Gaussian fit have been plotted as a function of energy for Ba-133, Cs-137 and Co-60. A curve has been fitted to the results and they are displayed in Figure 5 (overleaf). Note that the FWHM as a percentage for Cs-137 (20 keV divided by 662 keV) is equal to 3%, which is what would be expected from the LaBr3 detector. Typically, an NaI detector would have a FWHM at this energy of between 7% and 8%.
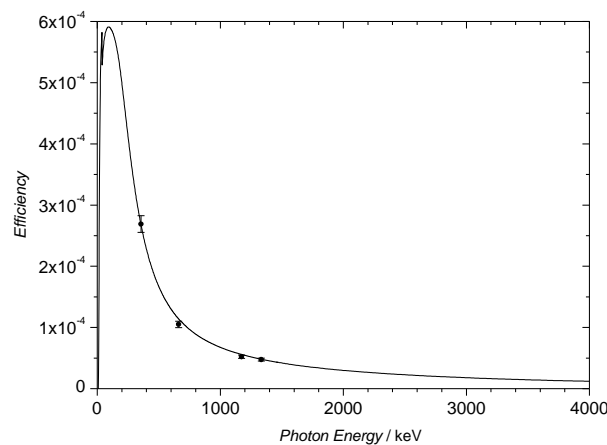

Figure 4. Detection efficiency as a function of photon energy for an isotopic point source.
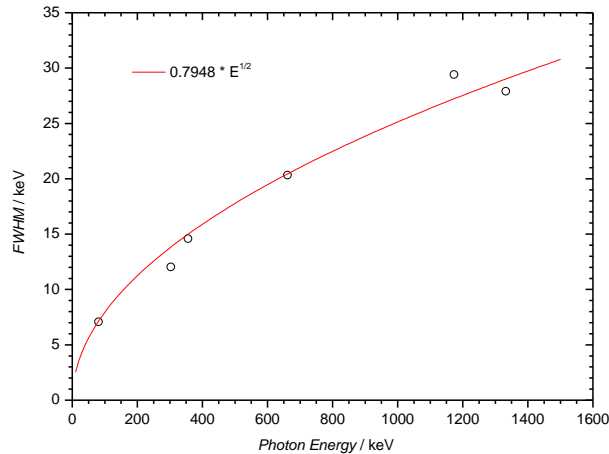
Figure 5. Experimental results for the FWHM as a function of photon energy. The data points are from Gaussian fits to the various peaks from Ba-133, Cs-137 and Co-60 point sources.

SCAN PROCESS ANALYSIS AND MEASUREMENT VERIFICATION

The scan process is based on a rectangular grid scan of an area or object, which is known as the Scan Area or Scan Grid. The Scan Area is divided into rectangular Scan Elements, each of which is either equal to or less than the detector field of view, either 4 degrees with the collimator barrel fitted or 18 degrees with the collimator barrel removed. At the beginning of the scan the camera captures a video image of the entire Scan Area. The pan and tilt mechanism then increments the detector head in a rectangular scan pattern or grid, viewing each Scan Element for a pre-selected measurement time, so that the detector obtains a gamma-ray spectrum corresponding to each Scan Element.

The process of scanning a surface has been studied and correction factors have been derived based on a Gaussian fitting process in order to determine the correct activity for a scanned area, considering that a single point source will contribute to the count rate measured for more than one Scan Element. This is particularly the case when the scan increment is less than the detector FOV. This process is illustrated in Figure 6 (overleaf), which shows the results of a 15 x 15 grid of Scan Elements measured with a 1-degree scan pitch. A point source has been placed at scan angle zero and the activity normalized to the activity of the source. The angle that is plotted is the effective angle for a combination of pan and tilt angles. A Gaussian function has been fitted to the data; this results in a FWHM angle of 3.88 +/- 0.09 degrees for the detector FOV. It can be seen that for under scanning, the source is seen to differing degrees at a variety of positions as the detector FOV moves across the source. Under scanning is defined as employing a scan increment or scan pitch angle that is less than the detector FOV.

Based on coefficients derived from the Gaussian fitting process, correction factors have been established, which take into consideration the under scanning effect and ensure that the total activity of the scanned area is correctly determined. This process has been tested using multiple point sources in a variety of configurations and using simulated distributed source data generated by an MCNP model. For scanning with the collimator barrel fitted, (effective detector FOV of 4 degrees), the effect of employing a variety of under scanning angles with variable distributed source area, is illustrated in Figure 7 (overleaf).
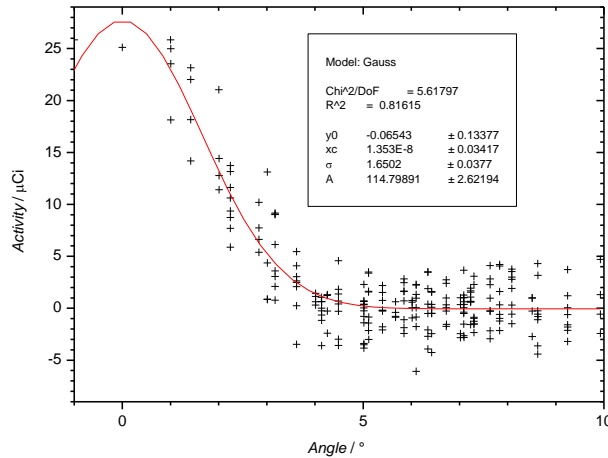
Figure 6. Gauss fit result to the data of a 15 x 15 scan with a 1° pitch (Scan ID 201206261102). The angle is the effective angle for a given combination of Pan and Tilt angles.
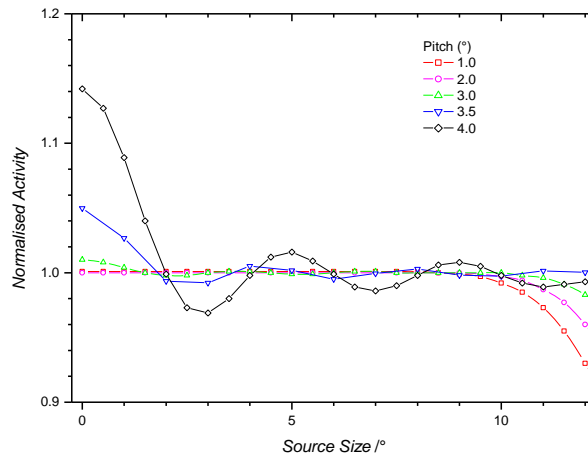

Figure 7. Simulated measurement of normalised activity as a function of uniformly distributed activity. The Source Size angle represents the extent of the uniformly distributed source.

Figure 7 presents simulated measurements of normalized uniform activity as a function of source size (represented by angle) for different scan pitch angles. Note that at a scan pitch angle of 4 degrees, corresponding to the detector FOV, an error of 15% is observed for the measurement of a single point source. For practical scanning, a scan pitch angle of 3.5 degrees was selected as this represented a good compromise between reduced scan time and acceptable measurement errors (5% for a point source). Note also that for scan pitch angles of less than 3.5 degrees errors arise from edge effects if the scan area and the area of activity correspond to one another in size.

Two examples of the operation of the scanning algorithm can be seen in Figures 8 and 9 (overleaf) for the measurement of Cs-137 point sources. In Figure 8 the equivalent of a single point source is measured with a scan grid of 15 x 15 and a scan pitch of 1-degree, at a distance of approximately 2 meters. In Figure 9 two equivalent point sources are measured, in this case with a grid of 7 x 5 and a scan pitch angel of 3.5 degrees at a distance of 2 meters. In both cases, the results agree within the measurement errors, corresponding to a 95% confidence interval. The figures show the overlay images produced by the analysis process.
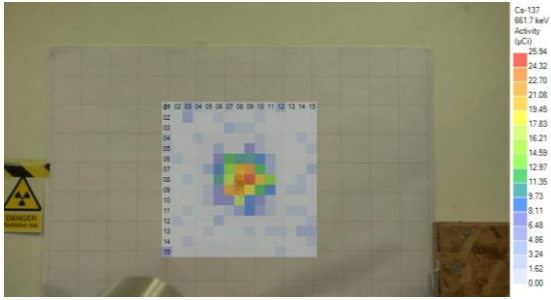
Figure 8. Scan overlay image for a scan with the stack of 4 Cs-137 sources (28.18 µCi) placed in the centre of the scan area. MCA pre-set time 60 seconds, scan grid 15 x 15, scan pitch 1°. Rangefinder distance 1.984 m. Scan correction factor is 0.059. Result for Cs-137 activity: (26.2 ± 4.0) µCi (95%, 2σ).
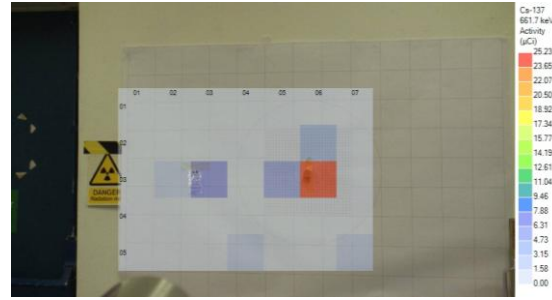

Figure 9. Scan overlay image for a scan with the stack of 4 Cs-137 sources (28.18 µCi) and the Cs-137 card source (9.025 µCi) placed arbitrarily on off-grid positions (total activity 31.21 µCi. MCA pre-set time 400 seconds, scan grid 7 x 5, scan pitch 3.5°. Rangefinder distance 1.999 m. Scan correction factor is 0.715. Result for Cs-137 activity: (33.3 ± 7.8) µCi (95%, 2σ).

The measurements illustrated in Figures 8 and 9 are tabulated with other point source measurement data in Table 1 (overleaf). In the table, the reference activity is quoted as is the measured value with associated error [3]. In all but one case, the deviation is within the 95% confidence interval. It should also be noted that all of the results are for small sources where the counting statistics are limited and larger errors are expected in these cases.

The effect of counting time on the errors is illustrated in Figure 10. The measurements presented in this figure are also included in Table 1. In order to verify the scanning process two point sources, arbitrarily located on the surface, were measured repeatedly with a 7 x 5 scan grid and a 3.5 degree scan pitch, at a distance of 2 meters. It can be seen that both the measurement precision and measurement accuracy improve as the count time increases.
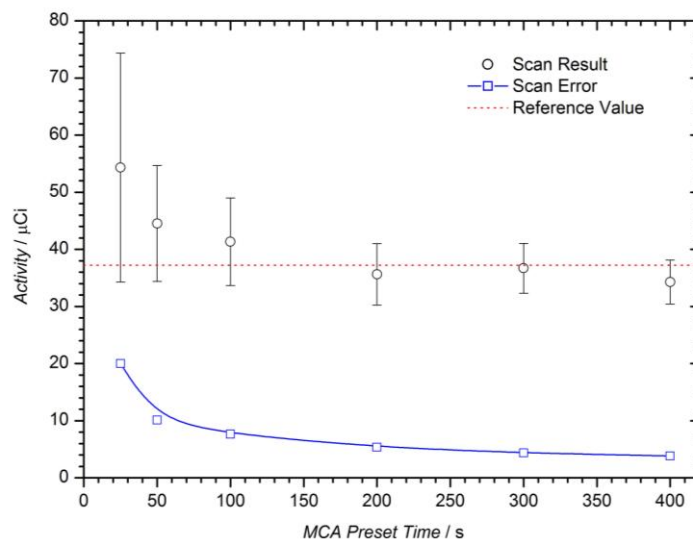

Figure 10. Results of repeated verification measurements of the same source distribution and the same scan grid for various different measurement times.

Scan ID	Pan	Tilt	Pitch (°)	Range (m)	MCA Time (s)	Total Scan Time	C_f	Scan Result Cs-137 Activity (µCi)		Ref. Activity (µCi)	Deviation	Exp. Error
								Value	Error 2 sigma			
201206261102	15	15	1	2	60	225	0.059	26.2	4.0	28.2	-7%	15%
201206271515	5	5	2	1	320	133	0.236	28.0	0.9	28.2	-1%	3%
201207131704	7	5	3.5	2	25	15	0.715	29.8	31.7	37.2	-20%	106%
201207131618	7	5	3.5	2	50	29	0.715	46.9	21.1	37.2	26%	45%
201207130815	7	5	3.5	2	100	58	0.715	42.7	15.5	37.2	15%	36%
201207131003	7	5	3.5	2	200	117	0.715	41.2	10.8	37.2	11%	26%
201207111516	7	4	3.5	2	300	140	0.715	35.4	8.0	37.2	-5%	23%
201207121002	7	5	3.5	2	300	175	0.715	37.2	8.9	37.2	0%	24%
201207131207	7	5	3.5	2	400	233	0.715	33.3	7.8	37.2	-10%	23%
201206291430	11	5	4	2	120	110	0.940	32.8	22.8	28.2	16%	70%
201206291011	12	6	4	2	120	144	0.940	58.8	25.7	28.2	109%	44%
201207111115	5	3	4	2	300	75	0.940	43.0	7.9	37.2	16%	18%
201207101549	3	3	4	3	300	45	0.940	19.2	12.6	28.2	-32%	66%

Table 1. Results of total activity measurement for a variety of scans of Cs-137 point sources.

MEASUREMENTS IN THE ALPHA GAMMA HOT CELL FACILITY AT THE ARGONNE NATIONAL LABORATORY

Scanning measurements of distributed radioactivity were performed around and looking into the Alpha Gamma Hot Cell Facility (AGHCF) at the Argonne National Laboratory (ANL). The measurement campaign represented the first practical deployment of the ANTECH RadSearch instrument in a radioactive environment. The instrument was used to measure distributed radioactive sources and to determine surface activity and identify and quantify different radionuclides distributed within the hot cell.

Figure 11 shows the RadSearch instrument deployed at AGHCF to measure radioactive holdup in a HEPA filter. The result of the measurement, showing the scanned grid overlaying the video image of the HEPA filter, is shown in Figure 12. At a range of 3.1 meters Cs-137 activity of 4.2 mCi was measured within the HEPA filter.

Figure 11. RadSearch measurement in the AGHCF at Argonne National Laboratory. A strong Cs-137 peak and Compton down-scatter are clearly visible in the spectrum displayed on the notebook computer.
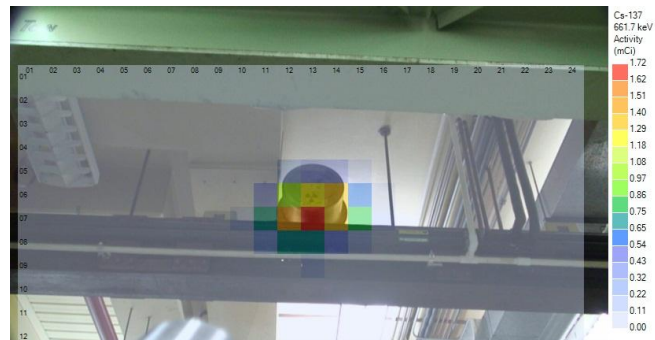

Figure 12. Scan of an internally contaminated HEPA filter in the AGHCF at ANL. MCA pre-set time 180 seconds, scan grid 24 x 12, scan pitch 2°. Rangefinder distance is 3.1 m. Result for Cs-137 activity: (4.2 ± 0.5) mCi (95%, 2σ).

Figures 13 and 14 show the overlaid images for measurements of a steel pulley behind the Clean Transfer Area (CTA) inside the AGHCF. The measurements were performed with a scan grid of 4 x 4 and a scan pitch of 1-degree, and at a distance of 7.5 meters. They show respectively the activity of Cs-137 (27.4 mCi) and Am-241 (5.8 mCi). A measured spectrum for a Scan Element (pan 02, tilt 04) from the measurement shown in Figures 13 and 14 is displayed in Figure 15. Note the two highlighted regions of interest corresponding to the 59.5 keV gamma-ray photon from Am-241 and the 661.7 keV gamma-ray photon from Cs-137.
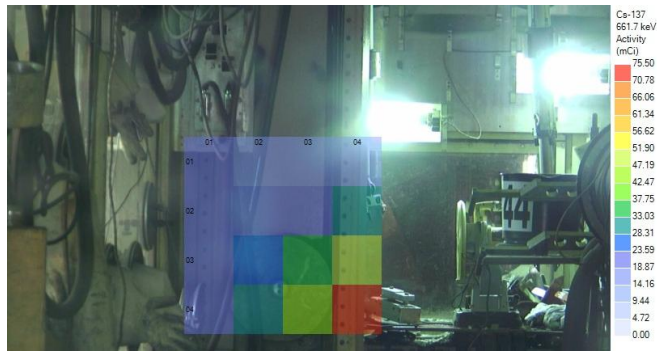

Figure 13. Scan of a pulley behind the CTA inside the AGHCF at ANL. MCA pre-set time 5 seconds, scan grid 4 x 4, scan pitch 1°. Rangefinder distance is 7.5 m. Result for Cs-137 activity: (27.4 ± 0.8) mCi (95%, 2σ).

Figure 14. Scan of a pulley behind the CTA inside the AGHCF at ANL. MCA pre-set time 5 seconds, scan grid 4 x 4, scan pitch 1°. Rangefinder distance is 7.5 m. Result for Am-241 activity: (5.8 ± 0.6) mCi (95%, 2σ).
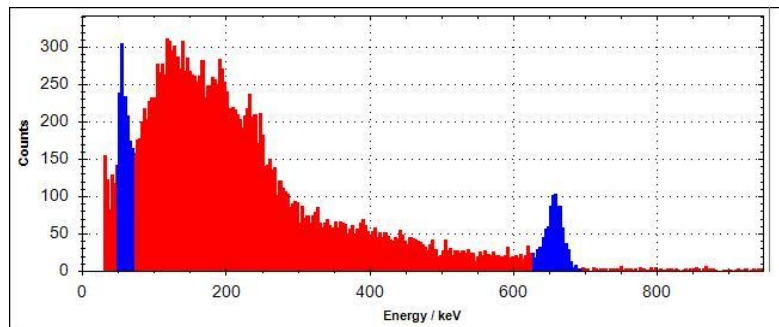

Figure 15. Spectrum of scan element (pan 02, tilt 04) of the previous two images from measurements in the AGHCF at ANL. Two regions of interest have been selected in the measured spectrum corresponding to Am-241 at 59.5 keV and Cs-137 at 661.7 keV. The higher than normal Compton background would suggest that the object (a metal pulley) is contributing to the Compton down-scatter.

A small drum containing a significant radioactive source was measured on the far side of the AGHCF area. As the source strength was significant, a pre-set scan time of 5 seconds was chosen with a scan grid of 10 x 6 and a scan pitch of 1-degree; the measurements were made at a distance of 14 meters. The Cs-137 activity of the container was measured as 72.6 mCi. The overlaid scan image is shown in Figure 16 (overleaf).
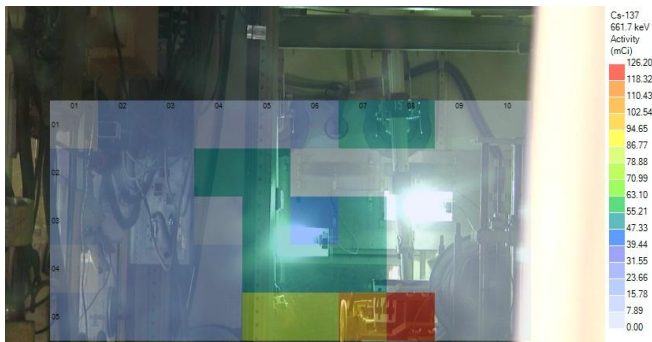
Figure 16. Scan of a small drum behind the CTA in the AGHCF at ANL. MCA pre-set time 5 seconds, scan grid 10 x 6, scan pitch 1°. Rangefinder distance 14 m. Result for Cs-137 activity: (72.6 ±2.4) mCi (95%, 2σ).

CONCLUSIONS

A variety of measurements have been made to establish and test the performance of the ANTECH RadSearch instrument for different source distributions and measurement distances. The Gaussian based correction factors established as part of this study have been confirmed and validated by these measurements employing single and multiple point sources on a test grid and by Monte Carlo simulations of distributed sources. Very good agreement has been obtained between point source measurements and MCNP simulations. Measurement errors have been within both an expected and acceptable range. Measurements with small point sources and data obtained from measurement of large sources at the Argonne National Laboratory show both the reproducibility of the results and the broad dynamic measurement range of the instrument.

REFERENCES

[1] J. F. Briesmeister, *MCNP - A General Monte Carlo N-Particle Transport Code (Version 4C)*, Los Alamos National Laboratory, LA–13709–M, 2000.

[2] Tables of X-Ray Mass Attenuation Coefficients and Mass Energy-Absorption Coefficients from 1 keV to 20 MeV for Elements Z = 1 to 92 and 48 Additional Substances of Dosimetric Interest, J. H. Hubbell and S. M. Seltzer, National Institute of Standards and Technology (NIST,) U.S. Department of Commerce, http://www.nist.gov/pml/data/xraycoef/index.cfm

[3] L. A. Currie, *Limits for Qualitative Detection and Quantitative Determination*, Analytical Chemistry, 40 (3), p. 586-593, March 1968.